CHAPTER 4

Electro-Mechanical Characterization of Ceramic Porcelain Insulator with Zirconia Reinforcement

4.1 Introduction

In this chapter, we use a ZrO_2 component for increasing the mechanical as well as electrical properties of ceramic porcelain insulator (CPI). Zirconia is one of the most valuable ceramic material and have attracted attention to industrial applications in oxygen pumps, sensors, fuel cells, and thermal barrier coatings due to its excellent electrical, mechanical, thermal properties and having high strength, low thermal conductivity compared to other ceramics [Tartaj et al. 1996, Wahsh et al. 2012 and Wan et al. 2015]. For CPI, the electrical insulation should have a high electrical resistivity that minimizes the energy conducted. In addition to electrical resistivity, other important electrical properties for ceramic porcelain insulator are the dielectric constant (ε'), loss tangent ($\tan\delta$) and dielectric strength (KV/mm). Dielectric is the property of a material that conducts electricity poorly or not at all. If the voltage is applied to a dielectric material, the atoms in the material arrange themselves in such a way as to oppose the flow of electrical current. A dielectric material, also known as an electrical insulator, gets polarized with the application of electric field. As a dielectric placed in an applied electric field, electric charges do not flow through the material as they do in a conductor because of dielectric polarization, positive charges are displaced toward the field, and negative charges shift in the opposite direction. Due to this, an internal electric field generated which further reduces the overall field in dielectric itself [Chaudhuri et al. 2000 and Di Marco et al. 2017]. Dielectric loss evaluates a dielectric material's inherent dissipation of

electromagnetic energy (e.g., heat). It can be parameterized regarding either the loss angle or the corresponding loss tangent (tanδ). Dielectric losses lead to heat evolution; losses occur due to chain motion because every change has to move in the same direction which may lead to sample destruction or shape change of material. Chain motion creates flow in structure due to which its properties can vary from its natural behavior. In the chapter, we are mainly concerned with the effect of alumina-zirconia (Al_2O_3–ZrO_2) mixtures in the dielectric behavior of the base composition of about the concentration of the existing phases. In previous chapter 3, we found that composition A3 and A4 give better results according to the mechanical and electrical point of view. So in this chapter 4, we take composition A4 as a base composition for Ceramic Porcelain Insulator and doing reinforcement of zirconia with replacing alumina concentration. This study aimed to analyze the structural, mechanical, thermal and the dielectric behavior of zirconia–alumina composites addition on the base composition of CPI were investigated. The analysis of dielectric constant and loss tangent of porcelains insulator at microwave frequencies with temperatures variation was done. The prepared samples with the change in the zirconia concentration are sintered at two different temperatures (1250 and 1350°C). The rate of increment in sintering temperature is kept constant for 5°C/minute to remove any discontinuity while sintering.

4.2 Experimental Material Preparation and Techniques

Four different CPI compositions were prepared by increasing amounts of ZrO_2 concentration in a base porcelain composition having Al_2O_3, SiO_2, feldspar, kaolin and ball clay as listed Table 4.1. The concentration of ZrO_2 was taken as 0, 10, 20 and 30 wt. % with replacing Al_2O_3, in a fixed other component of CPI base composition. The particle size of 120 μm of raw materials, i.e., feldspar, kaolin, ball clay were taken initially after

passing through 120 μm mesh sieve due to its hygroscopicity. Similarly ZrO_2, SiO_2 and Al_2O_3 having particle size 80 μm obtained by passing through 80 μm mesh sieve. The particle size distribution of raw materials was recorded as shown in Table 4.2

All chemical powder passed through the mesh sieve to reduce the size of the agglomerates before compaction. Here we prepared a 100 gram for each composition according to the batch formulation (S1, S2, S3, and S4), then took it in agate and hand mixing was done using pestle for 1 hour. Further, detailed experimental procedure disscussed in chapter 2. Each sample having a dimension of circular 30 mm (diameter) and rectangular (40x10x10 mm) was prepared by pressing for a constant period of 10 minutes (holding time) at 160 MPa pressure. The different shapes of compacted samples thus formed were then sintered at temperatures 1350ºC with the rate of 5°C/minute (Figure 4. 1). Soaking time of sintering at peak temperature for each sample was 2 hours.

Table 4. 1: Shows the code for the formulation applied and the corresponding level of addition (taken in wt. %).

Samples	Ball clay	Kaolin	Feldspar	SiO_2	Al_2O_3	ZrO_2
S1	20	25	10	15	30	0
S2	20	25	10	15	20	10
S3	20	25	10	15	10	20
S4	20	25	10	15	0	30

Table 4. 2: Particle size distribution of raw material.

Raw Material	Kaolin	Ball Clay	Feldspar	SiO_2	Al_2O_3	ZrO_2
Particle Size (μm)	120	120	120	80	80	80

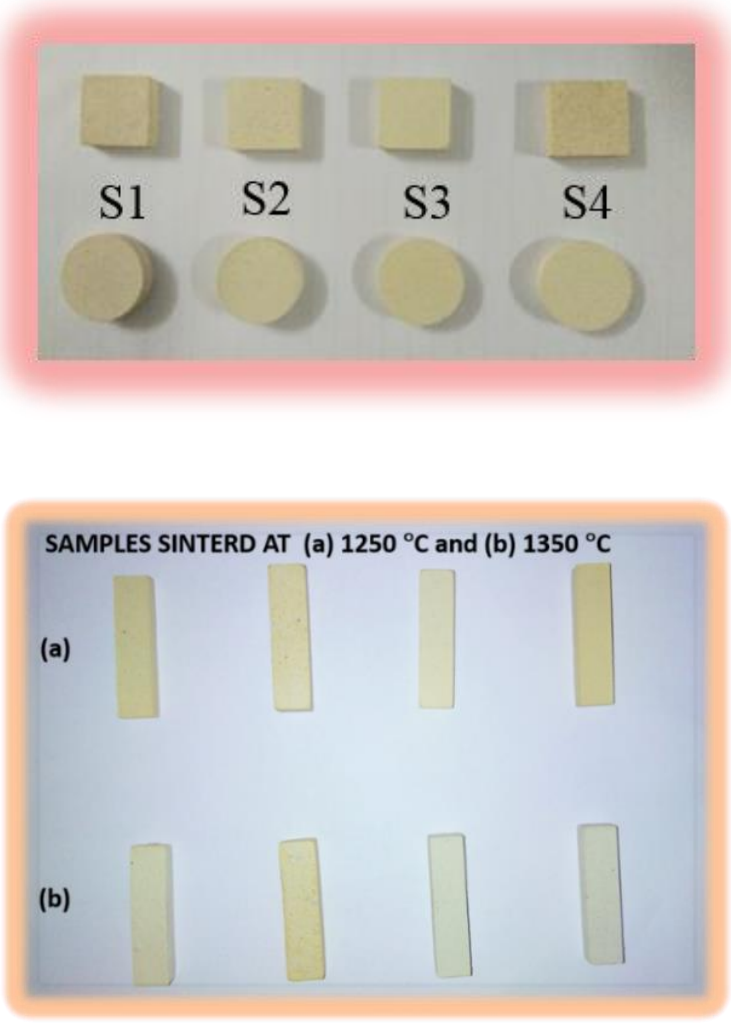

Figure 4. 1: Different shapes Samples sintered at different temperature (a) 1250°C and (b) 1350°C at the rate of 5°C/min with the soaking period for 2 hours.

4.2.1 Characterization

Various techniques were used to investigate the physical, mechanical, thermal and dielectric characteristic of sintered samples. For physical behavior such as apparent porosity and bulk density were determined by Archimedes method according to ASTM C20. The mechanical resistance such as; bending or modulus of rupture (MOR), compressive strength and tensile strength of the sintered samples of different compositions measured by using the Universal testing machine (UTM). The tensile strength of each composition was measured using a universal testing machine (UTM)) at strain rate 2 mm/min at room temperature. Four samples at least for each composition were prepared and sintered under the same conditions, and an average value was taken. Samples were having dimension 25 mm gauge length, 7 mm width, 10 mm thickness and 40 mm overall length. The tested rectangular specimen is compressed between two flat plates. The following relation gives its tensile strength:

$$\sigma_t = F / A$$

Where σ_t (MPa) is the maximum tensile stress, F (N) is the applied load at fracture, A (mm^2) is the cross-sectional area.

For measurement of the physical behavior of the various samples were carried out by Archimedes method according to ASTM standards. The water absorption, apparent porosity and bulk density of prepared sintered samples are were calculated by using the following relation:

$$\text{W. A (in \%)} = \frac{w_w - D_w}{D_W} \text{ X } 100$$

$$\text{A. P (in \%)} = \frac{w_w - D_w}{w_w - S_W} \text{ x } 100$$

$$\text{B.D (in gcm}^{-3}) = \frac{D_W * \rho}{w_w - S_W}$$

Where ρ is the density of water, w_w the wet weight which is measured after is kept the samples in a water bath for 5 hours at 80°C, D_w is the dry weight of the samples, and S_W is the suspended weight of samples in a water bath.

The samples linear shrinkage is determined by calculating the dimensions of the sample before (initial length) and after sintering (final length).

$$\text{L. S (in \%)} = \frac{\text{initial length} - \text{final length}}{\text{final length}} \text{ X } 100$$

The sample for the thermal expansion experiment having a dimension (40x10x10 mm) is required. The linear thermal expansion coefficient is measured from ambient temperature to 1300°C. The formula for linear expansion coefficient is:

$$\alpha_L = \frac{\Delta L}{L \Delta T}$$

Where L is the length of the test sample in ambient temperature, ΔL is the increased length of the test sample from ambient temperature to 1300°C, ΔT is the increase in temperature. Thermal expansion study of each pellets having a dimension (40 mm x10 mm x10 mm) was carried out by dilatometer (M/s V.B Ceramics and consultant, Chennai, India).

Phase analysis was done using a Rigaku high-resolution powder X-Ray Diffractometer (XRD) Cu-Kα radiation, λ= 1.540598 Å (Serial no: HD20972, Rigaku Corporation, Tokyo, Japan). The data collected at a scanning rate of 5°/min for 2θ in a range from 10° to 80° and comparing the diffraction patterns with the JCPDS files. The microstructure and composition of sintered samples were studied by scanning electron microscopy

(SEM) and energy dispersive spectroscopy (EDAX) using (Zeiss Company Model No. Evo\18-2045). Differential thermal analysis (DTA) and thermo gravimetric analysis (TGA) was performed on the prepared porcelain powdered composition from room temperature to 1350°C with a heating rate of 50°C/min, using instrument TG/DTA, Perkin Elmer India (P) Ltd. (LABINDIA).

For electrical measurements, the sintered samples were polished using the polishing machine to obtain a parallel surface and these sample placed between the two parallel plates. Samples are having a thickness of ≤ 2 mm and diameter of ≤ 10 mm were used for the experiment. Samples were coated on both sides with silver paste to form two electrodes. The relation between capacitance, dielectric permittivity, and geometrical dimension has been shown in eqation below.

$$C = \frac{\varepsilon o \varepsilon r' A}{t}$$

Where ε_o is permittivity of free space (8.85 X 10^{-12} F/m), ε_r' is real relative permittivity, A is the area and t thickness of the samples (Kingery, 1976 and Bartnikas, 1987).

Figure 4. 2: An instrument Impedance network analyzer used for measuring electrical characterization at operation frequency (20 Hz to 1MHz).

The electrical properties such as real relative permittivity (ε_r'), loss factor (ε_r''), loss tangent ($\tan\delta$), AC conductivity (σ_{ac}) and resistivity (ρ_{ac}) were measured using an Impedance network analyzer (Keysight Technology, model-E4990A, Malaysia) in frequencies range of 20 Hz to 1 MHz shown in Figure 4.2.

The dielectric constant (ε_r) and the dielectric loss ($\tan\delta$) of sintered samples were calculated concerning different values of temperature and frequency (4-20 GHz) using an instrument vector network analyzer Keysight E5071C ENA. The linear thermal expansion coefficient (α_L) for different samples was studied by dilatometer.

The AC dielectric strength of different sintered samples (S1, S2, S3, and S4) is measured using test setup supplied by NPTL Neo Tele Tronix Pvt. Ltd. Kolkata. The schematic diagram is shown in Figure 4. 3. Dielectric strength measurement is carried out following ASTM 2017 standard D149-97a. The test set up consists of two spherical electrodes with a diameter of 10 mm. Samples (with thicknesses of 1.2 mm to 1.5 mm, and diameter of 15mm) is inserted between two spherical electrodes. The voltage applied across the specimen is raised gradually (at the rate of 1kV/s) till sample fails. In order to avoid any surface flash over, the sample electrode assembly is submerged in transformer oil. The conducting test in oil bath is a better option than making recessed sample, which is more complex and time consuming especially when large numbers of samples are to be tested. In order to eliminate the effect of surface topography on breakdown data, electrodes and samples are properly polished and conditioned before conducting the test. If diameter of electrodes is D, and electrode spacing is S, a nearly uniform field between the two electrodes can be obtained if $S \leq 0.5D$. In this work diameter of spherical electrodes is 10 mm and the sample's thickness (S) lies between 1.2 mm to 1.5 mm. With these

dimensions of electrodes and samples, it is reasonable to assume electric field at the failure site is equal to average field i.e. E=Applied voltage (V)/ Sample thickness (S).

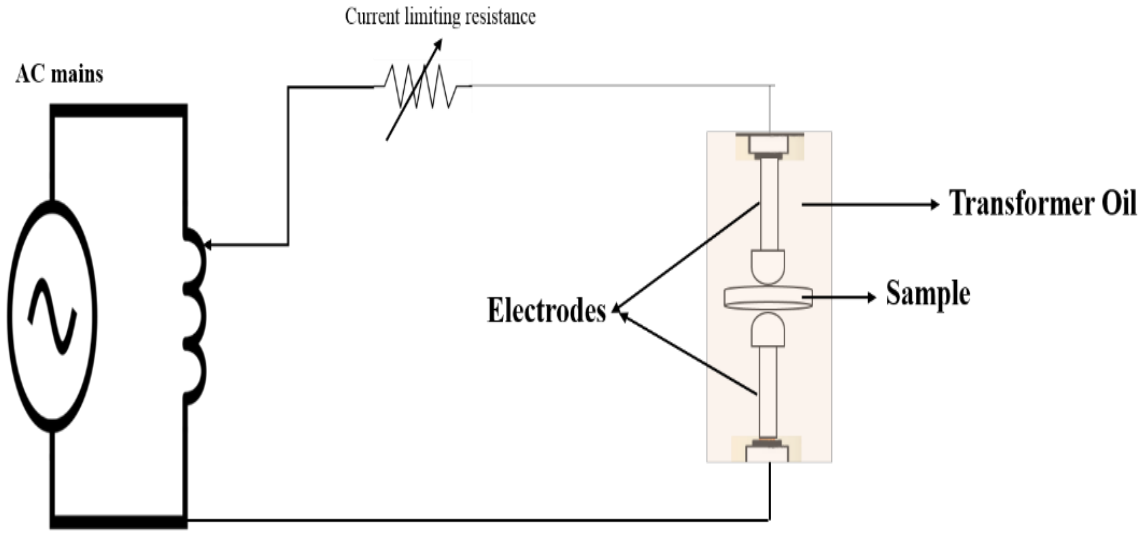

Figure 4. 3: Schematic diagram for AC dielectric strength measurements

4.3 Result and Discussion

The raw materials used in the experimental technique are ball clay, SiO_2, kaolin, feldspar, Al_2O_3, and ZrO_2. The samples prepared by solid-state reactions sintering process, sintering process reduced the sizes of pores that lead to a density of the green body (unfired samples). Solid-state sintering takes place between particles of single or various phases, where homogenization takes place during the sintering of mixed phases that form a single-phase product [Krupa and Malinaric, 2015 and Kasrani et al., 2016]. Figure 4. 4, TGA measurements reveal that dehydration and dehydroxylation are the only sources of weight loss during sintering. In the sample S1, the weight loss observed initially, around 110℃ for the S1 and 120℃ for samples S4, this peak is attributed to the vaporization of the physically adsorbed water molecules within the samples. In Figure 4.

4 (a), a broad endothermic peak is at ~550°C due to both clay dehydroxylation reaction and α-β transformation of quartz.

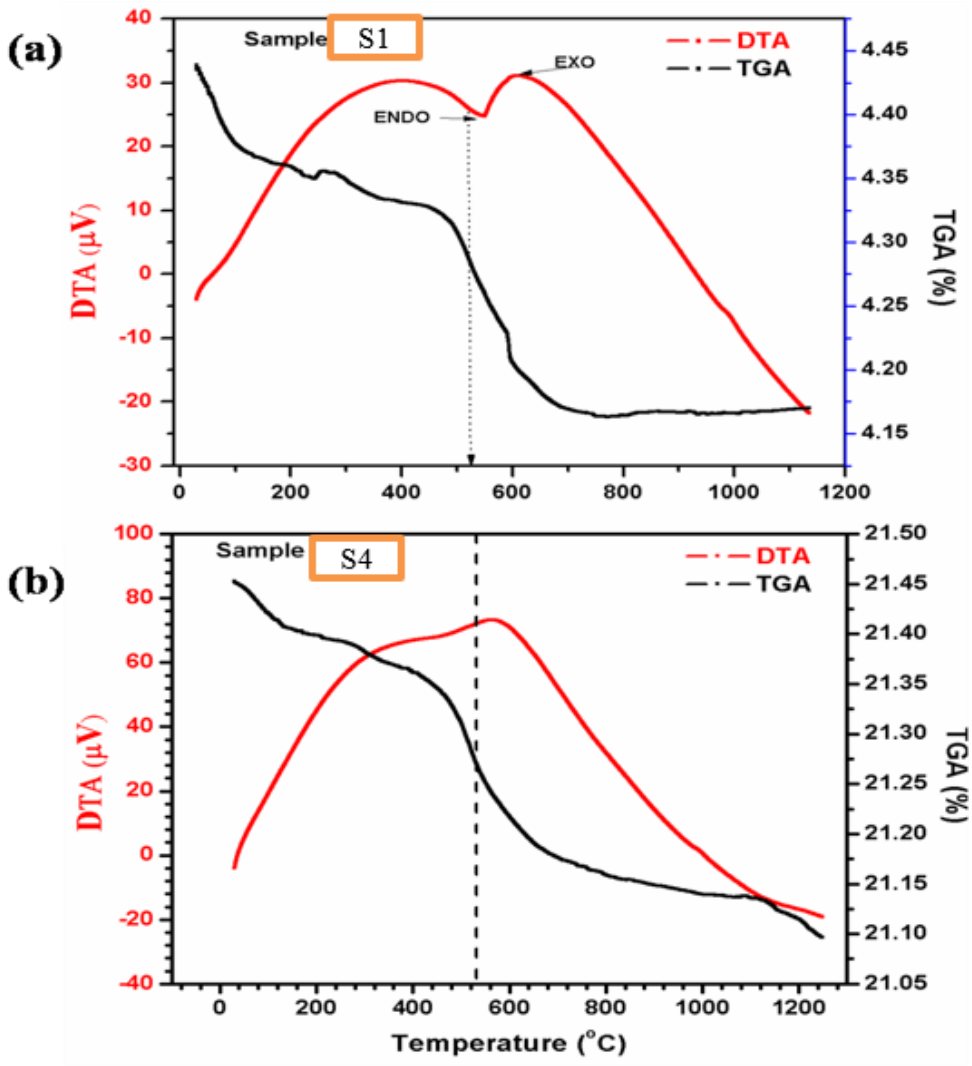

Figure 4. 4: DTA/TGA curves of different samples with heating rate of 50ºC/min (a) Sample S1 and (b) Sample S4

The weight loss associated to this endothermic is 4.40 %. A wide exothermic peak is seen to appear in between 600 and 630℃ for the samples S1. In the both composition samples above 800℃ (the end of dehydroxylation) curves are almost identical. For sample S4, an exothermic peak is seen and the weight loss between 460 and 670°C is due to evaporation

of structural water introduced during milling and release of binder. Additional exothermic peak seen at 1130℃ which is due to the crystallization of tetragonal zirconia (t-ZrO_2). The phase transformation from metastable tetragonal to monoclinic ZrO_2, generally observed in zirconia powders in the range 600 to 1000°C. Above 1100℃ it is well known that the stable phase is the tetragonal [Tartaj et al., 1996].

The XRD patterns of coded samples S1, S2, S3 and S4 sintered at 1350°C with 2 hours soaking time are recorded as shown in Figure 4. 5. X-ray diffraction analysis was performed to identify the different phases formed during sintering listed in Table 4. 3. The diffraction patterns revealed the presence of Al_2O_3 (corundum), zircon ($ZrSiO_4$), β-Cristobalite, m-ZrO_2 and t-ZrO_2 phases were identified matched with JCPDS data cards. As the concentration of ZrO_2 increased and Al_2O_3 decreased, the major peaks intensity decreased at an angle (2θ) of 25°, 35°, 43°, 52, 57 and 68°corresponding to alumina (©) because at high temperature the dissolution of alumina in glassy phase. At the same time, the peak intensity of zircon enhances at an angle (2θ) of 26.9°.

Table 4. 3: Show the X-Ray Diffraction analysis to identified different phases formed during sintering at 1350°C.

Phases	**Peak Intensity (h, k, l)**	**2θ (Degree)**	**JCPDS DATA**
Al_2O_3	1, 0, 4	35.1	46-1212
β-Cristobalite	1, 1, 1	21.5	89-3435
Zircon ($ZrSiO_4$)	2, 0 ,0	26.9	83-1374
t-ZrO_2	0, 1, 1	30.2	50-1089
m-ZrO_2	1, 1, 1	28.1	65-1023

The estimation of particle size is carried out using Debye Scherer formula given by

$$D=\frac{0.9\lambda}{\beta cos\theta}$$

Where D is the particle size (crystallite size), β= Full width half maximum intensity (FWHM) of highest peak and λ is the wavelength of the X-ray. The crystallite size of the different sintered samples (S1, S2, S3 and S4) listed in Table 4. 4.

As we increase the zirconia concentration (0 to 30 wt. %) in base composition the peak intensity of β-cristobalite phase is going to decreases at angle (2θ) of 21.5° with h, k, l, values [1, 1, 1] having cubic structure with space group Fd3m. We have calculated the lattice parameter for samples as per β-cristobalite phase are 7.153 Å. At the surface the presence of zirconia results from the formation of ZrO_2 particles, as identified by peak at 2θ =30° and 50°, corresponding to the [111] and [220] of zirconia in a tetrahedral phase (JCPDS 50-1089).

Table 4. 4: Show the crystallite size of different samples.

Samples	**Peak intensity (2θ in º)**	**β**	**Crystallite Size D (nm)**
S1	21.5	0.258	0.547
S2	35.22	0.229	0.635
S3	27.1	0.161	0.889
S4	26.9	0.202	0.707

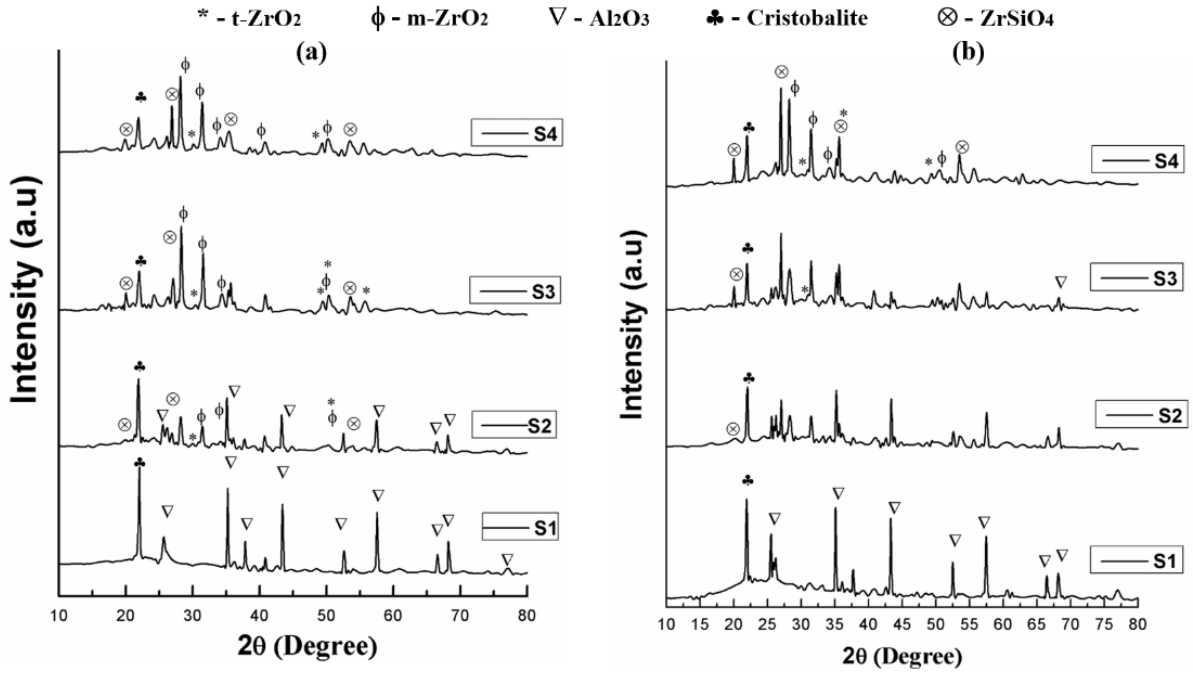

Figure 4. 5: The XRD patterns of a different sample containing (0 to 30) wt. % ZrO2 sintered at 1250 and 1350°C (where t-tetragonal and m-monoclinic).

The presence of a dispersed zirconium oxide metastable phase indicates the formation of an aggregation on the surface. The absence of mullite concurrently with the formation of m-ZrO_2 indicates that the rate of nucleation of m-ZrO_2 is higher than that of mullite. However, at high concentration of zirconia, the amount and the viscosity of the glassy phases may be suitable for the nucleation and crystallization of mullite and m-ZrO_2. As the increase the content of zirconia the intensity of the peaks for Al_2O_3 and ZrO_2 have been changed, the intensity of t-ZrO_2 increases whereas m-ZrO_2 phases decreases.

The surface morphology of four different compositions sintered at 1350°C is investigated using SEM/EDAX micrographs as shown in Figure 4. 6. The presence of little agglomeration and porosity in the sintered samples is confirmed by surface topographies. From SEM micrographs, it depicts the average grain size (S1=2.081μm, S2= 2.216 μm, S3=2.249 μm and S4= 3.413μm) of the different composition by using image J software.

Figure 4. ***6*** revealed that particles are in non-spherical shape and having little agglomeration with porosity. The temperature up to 1350°C reduces the agglomeration rate, less porous and non-uniform. As we increase the content of ZrO_2 up to 20 %, pores were probably disappeared because of pores filled by the glassy phase of silica. It may be justified with the increased density of the material, resulting enhancement in the mechanical strength. At 30 wt. % of ZrO_2 content, the mechanical strength is going to decrease. This is due to non-bonding additional free ZrO_2 content dispersed at the surface, results the close pores increases.

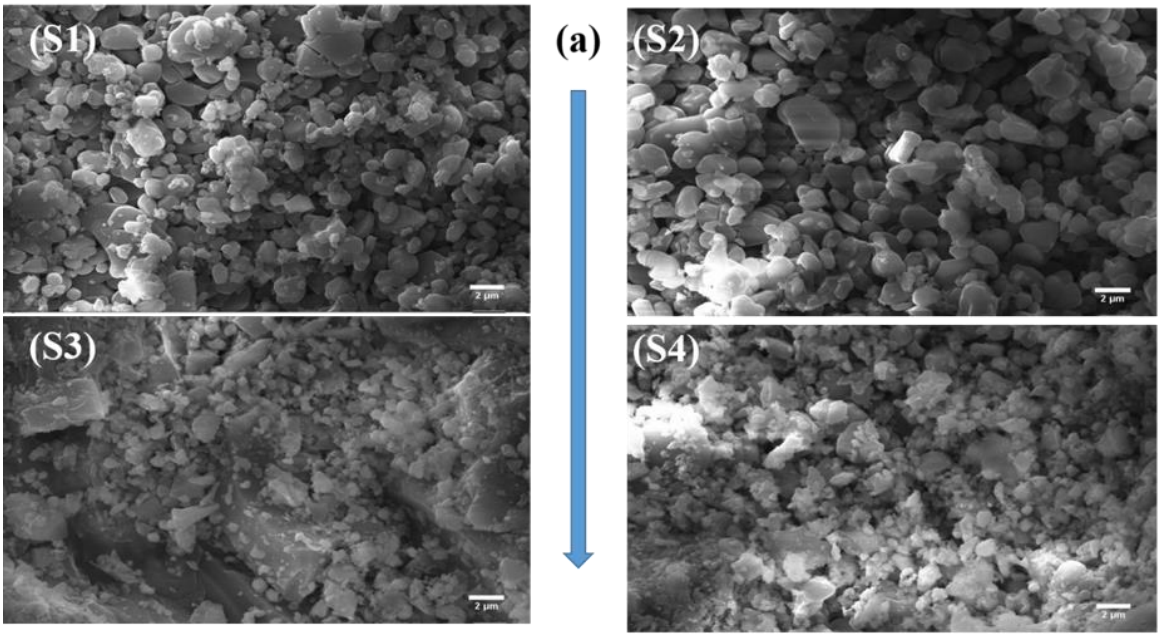

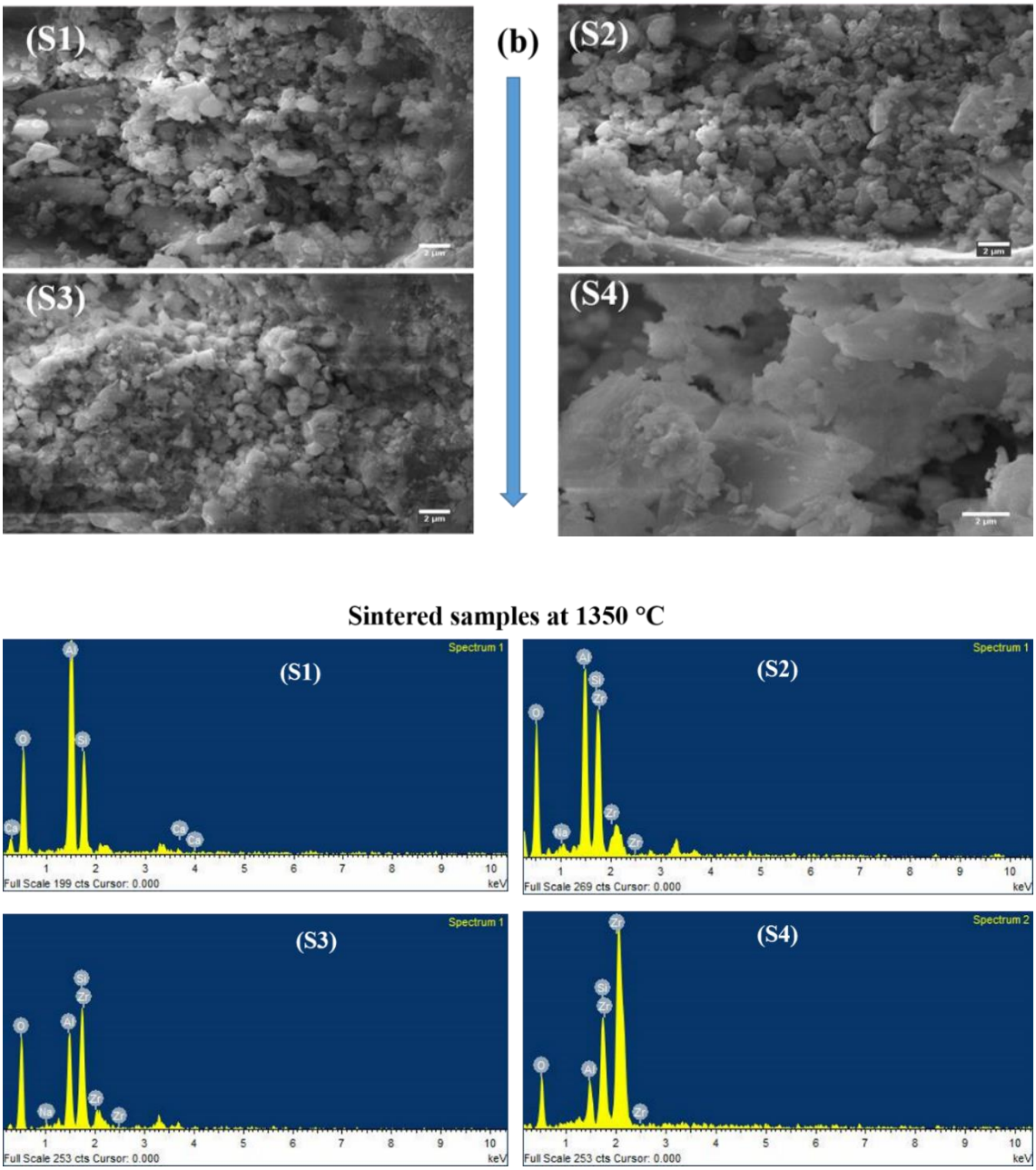

Figure 4. 6: SEM/EDAX analysis of different samples sintered at different temperatures with soaking time for 2 hours. (a) 1250°C and (b) 1350°C (where S1 = 0, S2 = 10, S3 = 20 and S4= 30 wt. % ZrO_2).

The thermal expansion of the different sample was determined in the range (30 to 1300°C) using dilatometer with sintering rate of 5°C/min from ambient temperature. For samples S2, S3 and S4 the heat-treated from 30 and 1300°C showed negative expansion up to 150°C followed by positiveexpansion up to 1100°C, showed thermal expansion

coefficient in the range of 10^{-6}. Sample S1 show positive linear expansion up to 1200°C but after addition of zirconia content its expansion goes to decrease (Figure 4. 7). As we know that zirconia is more insulating as well as having better mechanical and thermally resistant material. From Figure 4. 7, it reveals that the thermal expansion coefficient of the different composition decreases as we increase the concentration of zirconia concentration with reducing alumina content. Thermal expansion decreases due to increasing bond energy, which affects the melting point of solids, so high melting point materials to have lower thermal expansion. For samples S2, S3 and S4 it starts to melt approx. at 1000°C that result lead for densification.

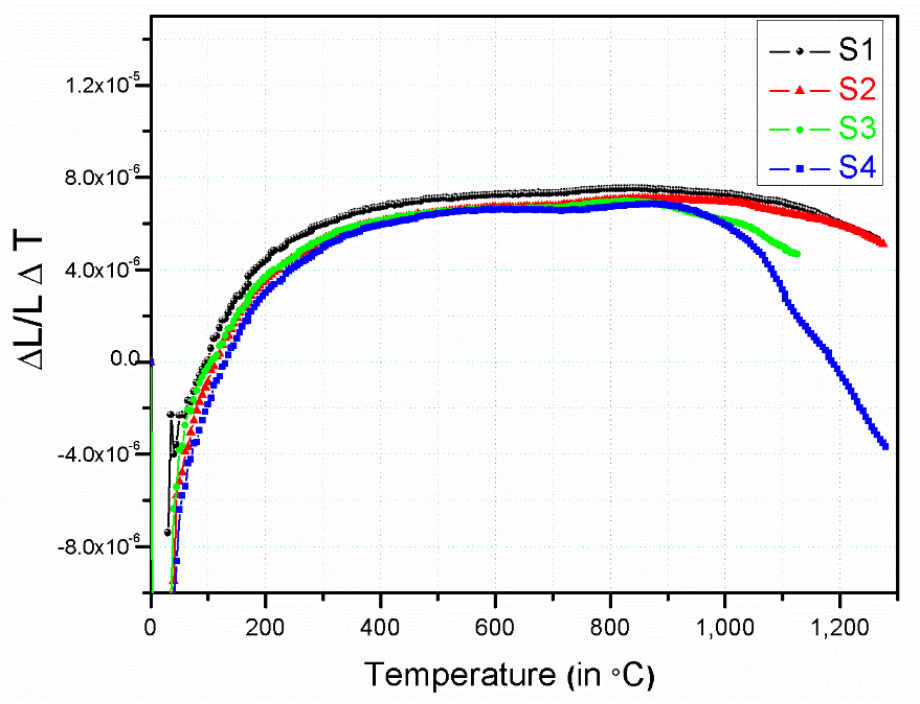

Figure 4. 7: Graph of Linear thermal expansion coefficient for different sintered samples with temperature.

4.3.1 Physical and Mechanical Properties:

Shown in Table 4.2 increase sintering temperature from 1250 to 1350°C with zirconia addition, the grain size of the particle increases due to ceramic particles connected closer

that influenced the linear shrinkage, porosity, and pore size significantly, which impact on densification of the resultant material. The result of physical properties (i.e., B.D in g/cm^3, L.S, W.A, and A.P are in %) at two different temperatures were listed in

Table 4. ***5***. Linear shrinkage of the sample increased with sintering temperature; sintering helps to fill up the inter-particles spacing result the volume goes to reduced. Water absorption and apparent porosity were also found to decrease with sintering temperature because of a decrease in microcrack and pores.

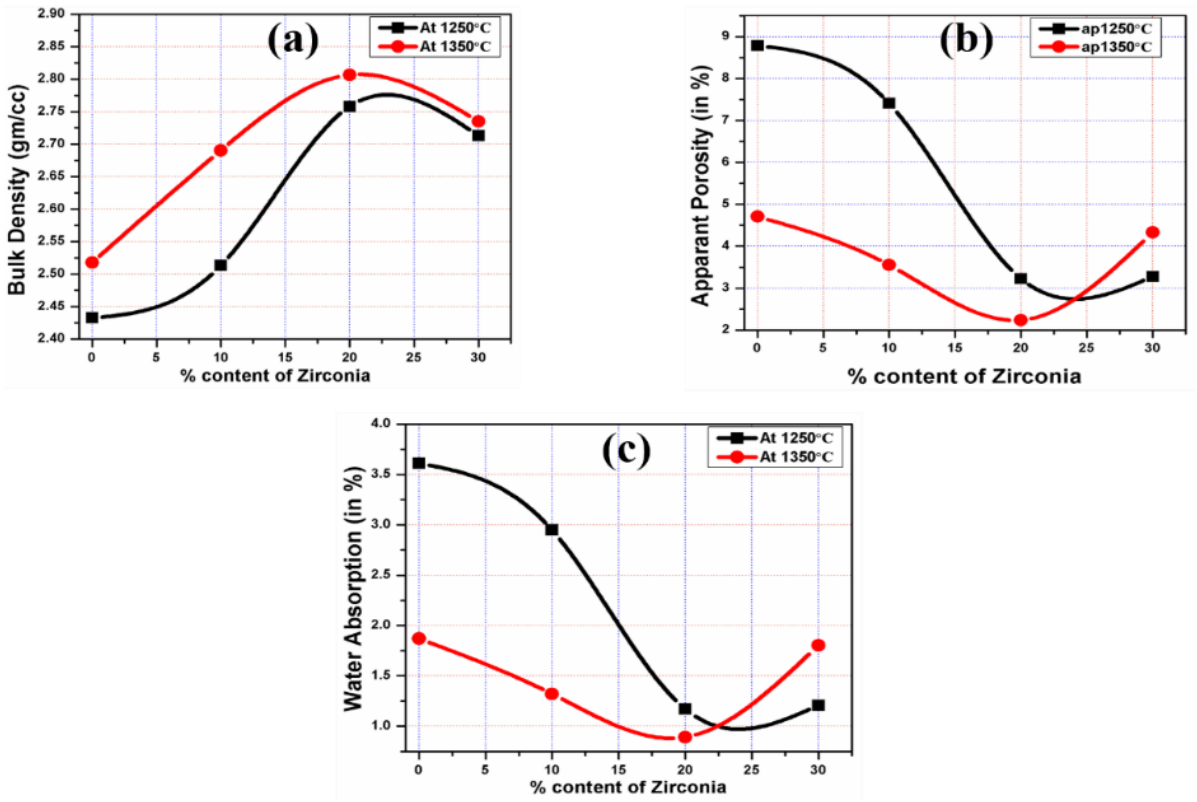

Figure 4. 8: Graph between B.D (in gm/cc), A.P (in %), and W.A (in %) with the content of zirconia (0 to 30%) of different samples composition sintered at 1250 and 1350°C with soaking time for 2 hours.

The water absorption for ideal high voltage insulator is zero, but which is not possible practically. The value of W.A must not exceed (>1%) for good ceramic porcelain

insulator. The A.P and W.A dropped to a minimum upon addition of zirconia (sample S3) which sintered at 1350°C having a soaking period of 2 hours, shown in Figure 4. 8 (b and c). At 1350°C, the average densification for all the sintered samples was 2.68 g/cm^3 and about 2.61 g/cm^3 at 1250°C is measured. From Figure 4. 8, it also depicts that as the temperature increase, the density goes to increases up to for sample S3 and these are due to increased consolidation with temperature result minimize pores in the samples.

Table 4. 5: The value of the change in L.S (in %), W.A (in %), A.P (in %) and B.D (in g/cm3) after addition of zirconia with different sintering temperatures.

	1250°C				**1350°C**			
Physical Properties	**A.P %**	**B.D (g/cm^3)**	**W.A %**	**L.S %**	**A.P %**	**B.D (g/cm^3)**	**W.A %**	**L.S %**
S1	8.78	2.46	3.61	6.90	4.71	2.50	1.87	7.90
S2	7.41	2.51	2.94	7.50	3.55	2.69	1.32	8.14
S3	3.23	2.76	1.17	9.47	2.23	2.81	0.89	10.6
S4	3.28	2.71	1.20	9.21	4.32	2.73	1.80	9.47

By sintering method, the grain boundaries eliminated through grain growth and reduced the sizes of pores that lead to a density of the green body (unfired prepared samples). It also verifies from XRD Figure 4. 5, that in addition to zirconia concentration in the base ceramic porcelain composition the peak intensity corresponding to β-cristobalite phase of silica decreases. Result direct impact on densification and strength of the resultant samples because of declines in microcracks. During the cooling process, there is phase transformation from β-phase to α-cristobalite phase, due to this time volume contraction occurred in the samples. At this time some micro-crack is produced in the samples. After

further addition of zirconia, it starts to decrease because of the increase in the number of closed pores in the electrical porcelain body Figure 4. 8.

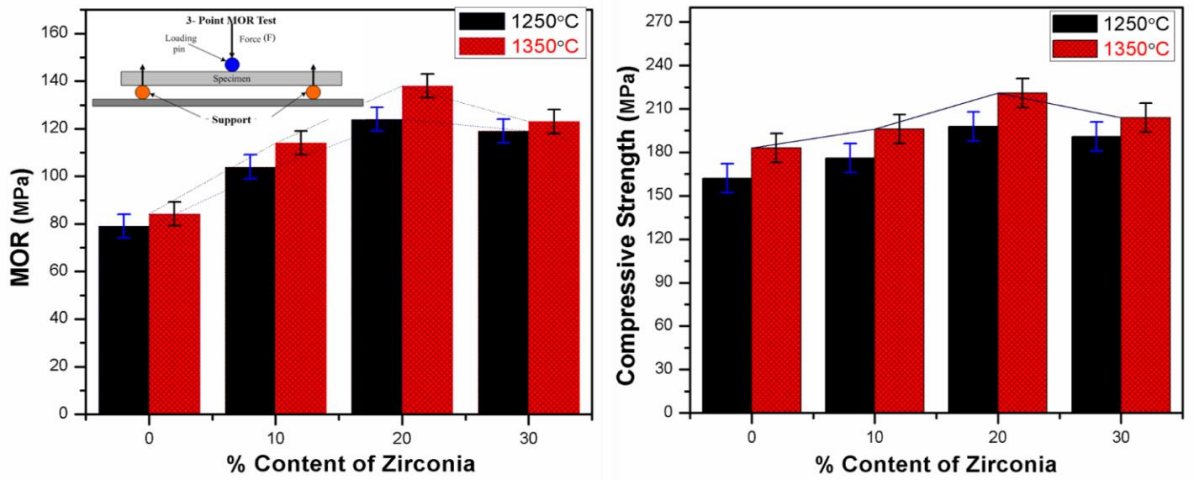

Figure 4. 9: Modulus of rupture (MOR) and compressive strength on the addition of zirconia (in wt. %).

In Figure 4. 9, investigated the behavior of the modulus of rupture and compressive strength with zirconia addition. The tests were done using the three-point bending technique. A rectangular sample is essential for the three-point bending test having a dimension (length 40 mm, breadth 10 mm and thickness 10 mm), shown in Figure 4. 9. The sample placed between the supports that are 40 mm apart, and a force applying in the middle of the two supports. MOR obtained using the formula:

$$MOR = \frac{3FL}{2bt^2}$$

Where F is the force (N), L is the distance between two supports, b is the breadth, and t is the thickness of the sample. The maximum value of the modulus of rupture (MOR) were observed for sample S3 (10 wt. % Al_2O_2 with 20 wt. % ZrO_2) was 124 ± 5 and 138 ± 5 MPa at sintering temperature respectively (1250 and 1350°C). From Figure 4. 9, it

reveals that on the addition of zirconia content the value of MOR gradually increases in sample S1, S2, and S3 but for sample, S4 goes to decrease. This result due to decline in densification because of increase open and close porosity in the samples shown in

Table 4. ***5***.

Table 4. 6: The calculated value of Modulus of rupture (MOR) and compressive strength of different samples with temperatures.

Zirconia (wt. %)	**MOR (MPa)**	**Compressive Strength (MPa)**	**MOR (MPa)**	**Compressive Strength (MPa)**
	1250 °C		1350 °C	
S1 (0)	79±5	162±10	98±5	183±10
S2 (10)	104±5	176±10	114±5	196±10
S3 (20)	124±5	198±10	138±5	221±10
S4 (30)	119±5	191±10	123±5	204±10

The graph of compression strength (in MPa) of ceramic porcelain insulator after increasing the content of zirconia (Figure 4. 9). It can measure by applied force against deformation in a testing machine. At 1350°C, the base porcelain composition sample (S1) without zirconia addition was maximum pressed 183 ± 10 MPa. After on addition of zirconia 20 wt. % with 10 wt. % alumina, it pressed at 221± 10 MPa. In samples due to variation in stress distribution the value of compressive strength in quite high the flexural strength (MOR).

For tensile strength measurement, we prepare four samples from each different composition (table 1). The densification was reflected on the mechanical properties of the samples S1–S4 sintered at 1350°C with soaking time of 2 hours are (Table 4.5). It is

observed that the increase of ZrO_2 concentration and sintering temperature are accompanied by a gradual increase in tensile strength from sample S1 up to S3 (Figure 4. 10). The Sample S3 sintered at 1350°C exhibited the highest tensile strength. The observed maximum strength for sample S3 is 41 ± 3 MPa at 1350°C. This may be due to the complete sintering and proper bonding between zirconia- alumina in addition to the presence of t-ZrO_2 content. ZrO_2 improves the mechanical strength through its decomposition on alumina and mullite crystals in which the solid state reaction could be completed at temperature 1350°C. The results of XRD confirm this. From XRD (Figure 4. 5) it prove that as we increases the ZrO_2 concentration the peak intensity at angle (2θ) of 21.5°, the β-cristobalite phase is going to decrease. Result the strength of the samples increases with decreases the micro cracks because during cooling, phase transformation from β-phase to α- cristobalite phase, due to this volume contraction occurred at this time, micro-crack is generated in the samples. After further addition of ZrO_2 for sample S4 it strength goes to decrease, due to the nonbonding remaining zirconia content results dispersed at the surface of samples which leads the porosity (Figure 4. 10).

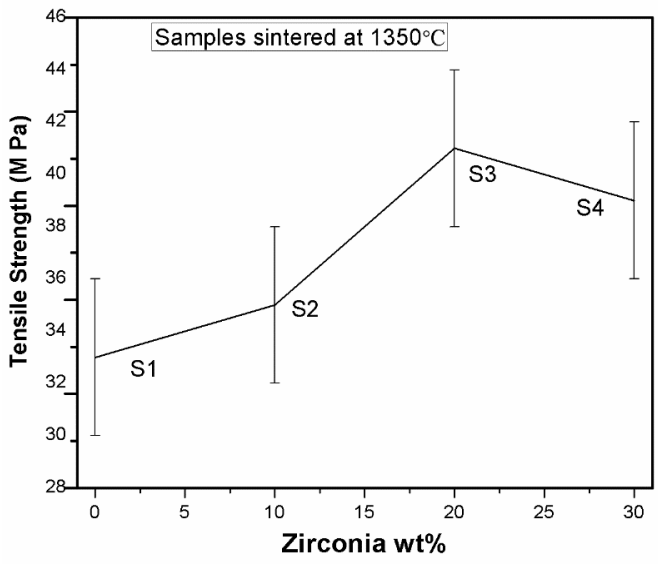

Figure 4. 10: Variation of tensile strength with the Zirconia (wt. %) content.

4.3.2 Dielectric Constant and Dielectric Loss at Room Temperature with Frequency Variation (20 Hz to 1MHz)

When dielectric materials are subjected to DC electric stress, the relative permittivity is a real number generally known as dielectric constant (ε_r).When dielectric materials are stressed with AC voltages, the relative permittivity is no more a real number but a complex number ($\varepsilon_r^* = \varepsilon_r' - j\varepsilon_r''$). The real relative permittivity (ε_r') is a measure of energy storage in the dipolar units, and imaginary relative permittivity (ε_r'') is related to dielectric losses and known as loss factor. The ratio of imaginary relative permittivity (ε_r'') to real relative permittivity (ε_r') is known as dissipation factor or loss tangent ($\tan\delta = \varepsilon_r'' / \varepsilon_r'$).

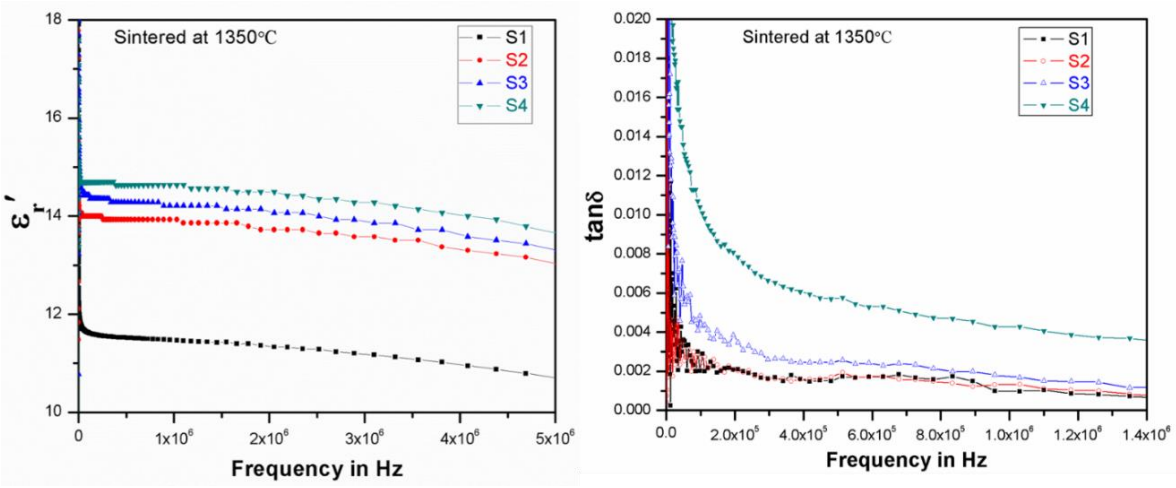

Figure 4. 11: Dielectric constant and dielectric loss versus frequency variation (Hz to MHz) at room temperature (30 °C) is investigated for different samples sintered at 1350°C.

Figure 4. 11, shows the measured values of real relative permittivity (ε_r') and dissipation factor ($\tan\delta$) as a function of frequency. The effect of increasing zirconia content (a maximum up to 30 wt. %) in place of alumina in the base PI is seen as an increase in the real relative permittivity (ε_r') and loss tangent ($\tan\delta$). The effect of frequency change on real relative permittivity (ε_r') and loss tangent ($\tan\delta$) is shown in Figure 4. 11. The

measured ε_r' values of sample S1, S2, S3 and S4 at 50 Hz are 14.85, 17.01, 17.78 and 21.35 respectively. Both parameters indicate a gradual decrease in their values with increase in frequency in the range of 20 Hz to 10^6 Hz. The decrease in above two parameters at higher frequency is possibly due to suppression of dipolar and space charge polarization.Figure 4. 12 shows loss factor (ε_r'') vs. frequency (f) characteristics. The decrease in loss factor is in good agreement with Debye relaxation theory (Al-Hilli et al., 2016).

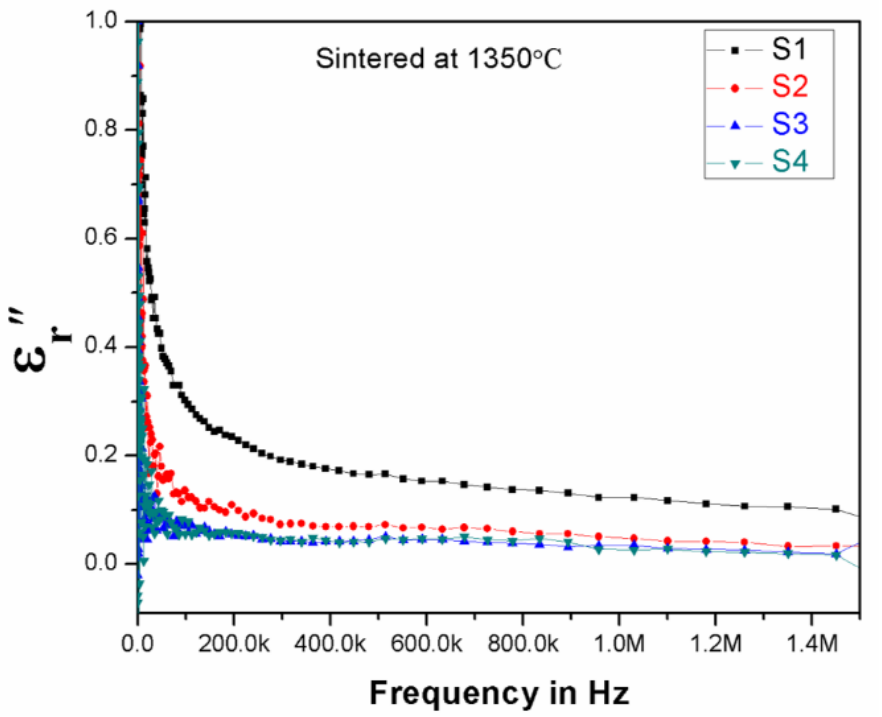

Figure 4. 12: Dielectric loss factor (ε″) versus frequency for the samples sintered at 1350°C.

4.3.3 AC Conductivity and Resistivity Measurement

AC resistivity ($\rho_{a.c}$) and conductivity ($\sigma_{a.c}$) is obtained using (ε_r'), (ε_r''), and tanδ, measured for a range of frequency 100 Hz to 1 MHz using Equation written below:

$$\rho_{a.c} = \frac{1}{\omega \varepsilon o \varepsilon''} = \frac{1}{\omega \varepsilon o \varepsilon' Tan\delta}$$

$$\sigma_{a.c} = \frac{1}{\rho a.c}$$

Where ω and ε_0 are angular frequency, and permittivity of free space respectively.

AC resistivity and AC conductivity vs. frequency characteristic for different samples are shown in Figure 4. 13. The steepness of characteristics gradually decreases with increase in frequency. At higher frequency, i.e., beyond 600 kHz, AC conductivity ($a_{.c}$) attains a steady value. As frequency increased beyond 600 kHz, the contribution to polarization from oriental and interfacial polarization decreases conductivity consequently becomes steady. AC resistivity being reciprocal of AC conductivity shows a reversal in characteristics obtained for AC conductivity.

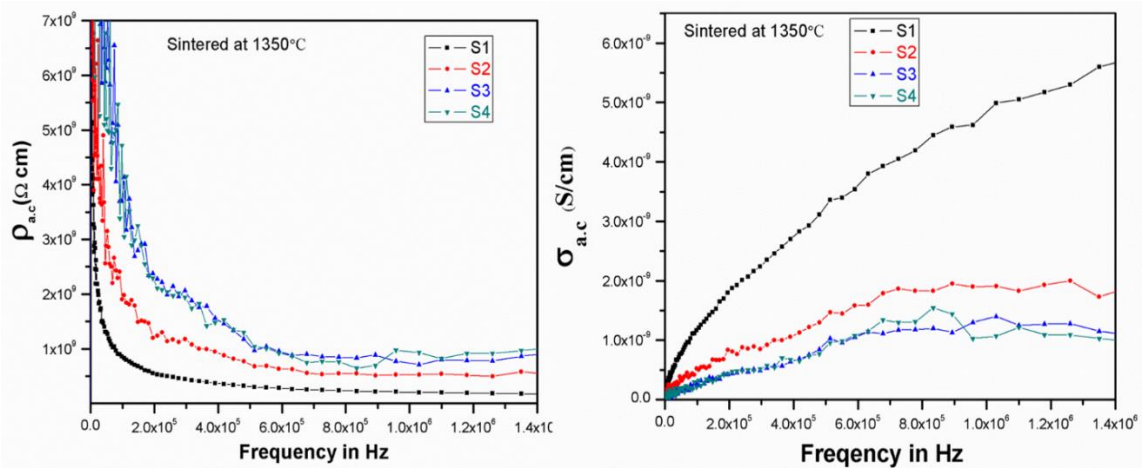

Figure 4. 13: AC electrical resistivity and conductivity versus frequency (in Hz) for all the sample sintered at 1350°C.

The average value of AC conductivity for all sintered sample at 500 Hz and 1MHz are 7.74×10^{-11} S cm^{-1} and 3.03×10^{-9} S cm^{-1} respectively. The effect of increasing zirconia content in PI causes a slight decrease in AC conductivity. Measured AC resistivity and conductivity for a range of frequency 100 Hz to 1MHz are shown in Table 4. 7.

Table 4. 7: The measured experimental value of an AC electrical resistivity ($\rho_{a.c}$) and conductivity ($\sigma_{a.c}$) of samples (sintered at 1350°C) with frequency variation (Hz to MHz).

AC electrical Resistivity (Ω cm)				
Frequency (Hz)	**S1**	**S2**	**S3**	**S4**
50	2.69E10	3.58E10	1.80E10	1.70E10
100	1.82E10	8.70E9	9.68E9	4.78E10
500	1.41E10	7.37E9	1E10	2.58E11
10^3	9.51E9	5.97E9	1.24E10	7.8E11
10^4	3.64E9	2.74E9	6.76E9	2.17E10
10^5	8.24E8	9.86E8	1.98E9	3.68E9
10^6	2E8	2.71E8	5.23E8	6.33E8
AC electrical Conductivity (S cm^{-1})				
50	3.71E-11	2.79E-11	5.55E-11	5.89E-11
100	5.49E-11	1.14E-10	1.03E-10	2.09E-11
500	7.08E-11	1.35E-10	1E-10	3.88E-12
10^3	1.05E-10	1.67E-10	8.06E-11	1.28E-12
10^4	2.75E-10	3.64E-10	1.48E-10	4.61E-11
10^5	1.21E-9	1.01E-9	5.05E-10	2.72E-10
10^6	5.05E-9	3.83E-9	1.83E-9	1.41E-9

4.3.4 AC Dielectric Constant and Dielectric Loss at Microwave Frequency

A dielectric material, also known as an electrical insulator, gets polarized with the application of electric field. The main properties of the electricalinsulation at high frequency are dielectric constant and dielectric loss or loss tangent (tanδ). Dielectric loss or loss tangent (tanδ) determine by using formula

$$\tan\delta = \frac{\varepsilon''}{\varepsilon'}$$

Where ε′a real part is called the dielectric constant, ε″ is imaginary part say the dielectric loss factor.

Table 4. 8: The experimental values of dielectric and loss (tanδ) values of different porcelain samples in Microwave Frequency.

	Measured at room temperature							
Frequency (GHz)	**ε′**	**tanδ**	**ε′**	**tanδ**	**ε′**	**tanδ**	**ε′**	**tanδ**
	S1		**S2**		**S3**		**S4**	
4	3.93456	0.02379	4.5081	0.08518	4.9959	0.08062	5.0989	0.08748
5	3.84922	0.08101	4.3184	0.08385	4.8622	0.07891	4.992	0.07071
6	3.87912	0.03485	4.3386	0.04598	4.8855	0.05424	5.0022	0.05196
10	3.60158	0.09877	4.0227	0.10205	4.5088	0.10198	4.6362	0.09682
20	3.46181	0.07748	3.7711	0.09517	4.3025	0.0985	4.3673	0.11715

As shown in Table 4. 8, it can be seen that as we increase the content of ZrO_2 (0 – 30 %), different samples sintered at 1350°C there is an increment in dielectric constant (ε′).The dependence of dielectric constant and dielectric loss (tanδ) on a different frequency at room temperature (Figure 4. 14). It also noted from Figure 4. 14 that, samples sintered at 1350°C having maximum values of dielectric constant is 5.0989 at 4 GHz and 4.3673 for 20 GHz for sample S4 at room temperature. Zirconia has ε′ of about 27, which is higher than that of alumina (≈10). So as forincreasing the zirconia content in the base composition ε′ goes to increases. The dielectric constant was observed to decreases in the high frequencies ranges (6 to 20 GHz), and dielectric loss was found to in the range of 0.018 to 0.13. A dielectric value depends on the presence of dipoles. If dipoles are there, then it would allow the flow of electrons to reduce the resistance hence small dielectric.As the material is dense, it offers more resistance to theflow so high is dielectric constant. At operating frequency of 6 GHz notable result comes, for each composition yield good

dielectric value and with minimum loss. As we know that the dielectric constant relies on mainly three types of polarization effects i.e. Ionic, orientation and electronic polarizations. Among them, ionic and orientation polarizability is slow to process contributes only up to frequencies 10^{10} Hz. The electronic polarization is only the fast process exists up to higher frequencies. In our measurement, at frequencies lower than 10^{10} Hz, both ionic and orientation polarization contributes making of dielectric constant to increase with frequency.

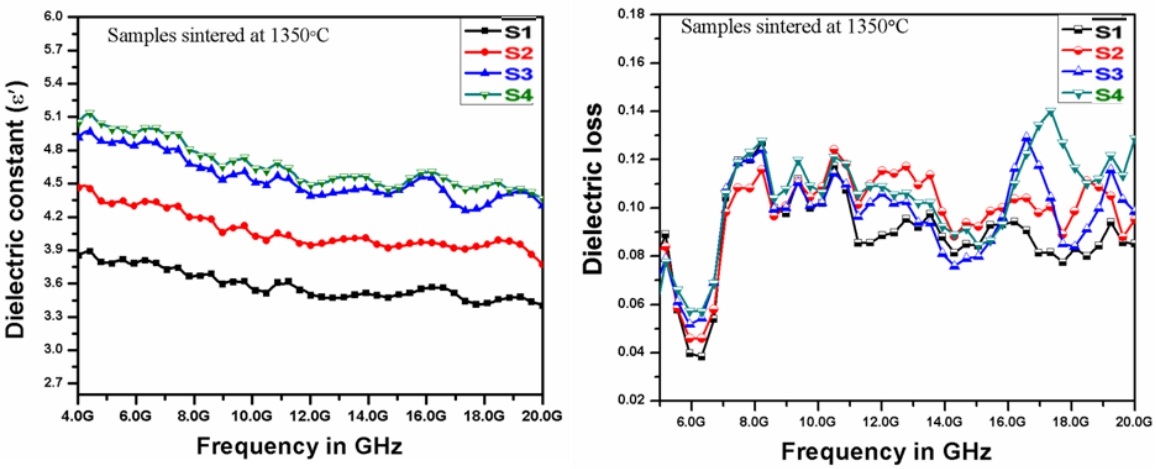

Figure 4. 14: Dielectric constant and dielectric loss versus frequency (GHz) at room temperature (30°C) is investigated for different samples sintered at 1350°C.

As we approach toward threshold boundary of frequency, i.e. ($4x10^9$ Hz -10^{10} Hz), only electronic polarization remains for the contribution which explains the decrease in dielectric constant after $0.6x10^{10}$ Hz (Kingery, 1976). In microwave range, the main problems are the rapid rise in dielectric loss factor. This thermal runaway is controlled by utilizing this electrical ceramic insulator composition. Due to its low dielectric loss and high dielectric value in microwave frequency, it might provide better insulation property.

4.3.5 AC Dielectric Constant and Dielectric Loss at 5 And 20 GHz with Temperature Variation

It is noted from Figure 4. 15 (a), the sample S4 having maximum AC dielectric constant values lie from 5.1 to 5.37 and dielectric loss from 0.10 to 0.11 at 5 GHz with temperature variation from 30 to 190°C. In Figure 4. 15 (b), the same sample having dielectric constant values lie in between 4.40 to 4.65 and dielectric loss from 0.12 to 0.15 at 20 GHz with temperature variation. The increase of ε' along with temperature was owing to the decrease of the bonding force between atoms at a higher temperature, which resulted in the increase of polarization. The increase of tan δ with temperature was attributed to the increase of electronic conduction loss, impurity ionic conduction loss and thermal defects conduction loss at a higher temperature.

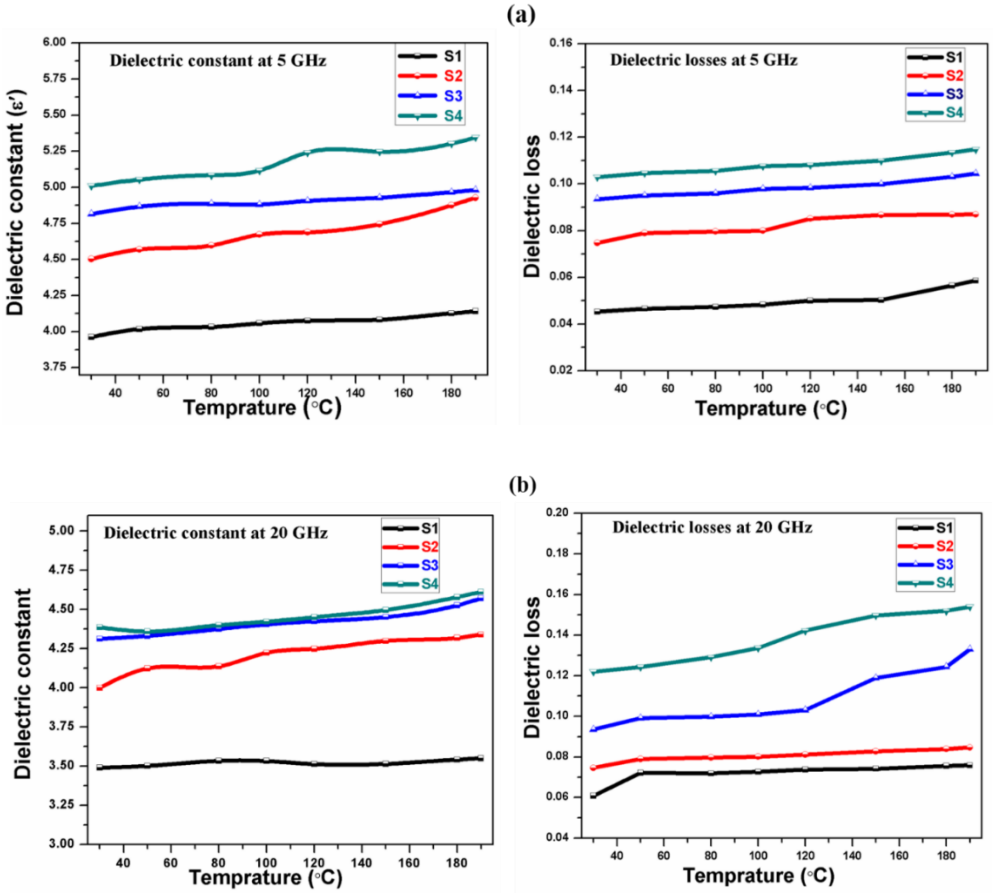

Figure 4. 15: Dielectric constant and dielectric loss versus temperature (30 to 190°C) is investigated for different samples sintered at 1350°C (a) For 5GHz and (b) 20 GHz.

4.3.6 AC Dielectric Strength Measurement

The average value of AC dielectric strength data is shown in Table 4.9. Figure 4. 16, reveals that the AC dielectric strength of prepared PI slightly increases with increase in zirconia content. The relative permittivity of zirconia is near about 27, which is much higher than that of alumina (≈ 10), resulting in high insulation property. The highest observed AC dielectric strength for samples S4 is 22.85 ± 0.5 KV/mm, which is sintered at 1350°C. It may be concluded that zirconia as a filler is effective in improving electrical properties.

Table 4.9: Measurement of dielectric strength of the different samples composition.

Sample	Breakdown Voltage (KV)	Dielectric Strength (KV/mm)
S1	26	18.57 ± 0.5
S2	27	20.77 ± 0.5
S3	27	22.40 ± 0.5
S4	31	22.85 ± 0.5

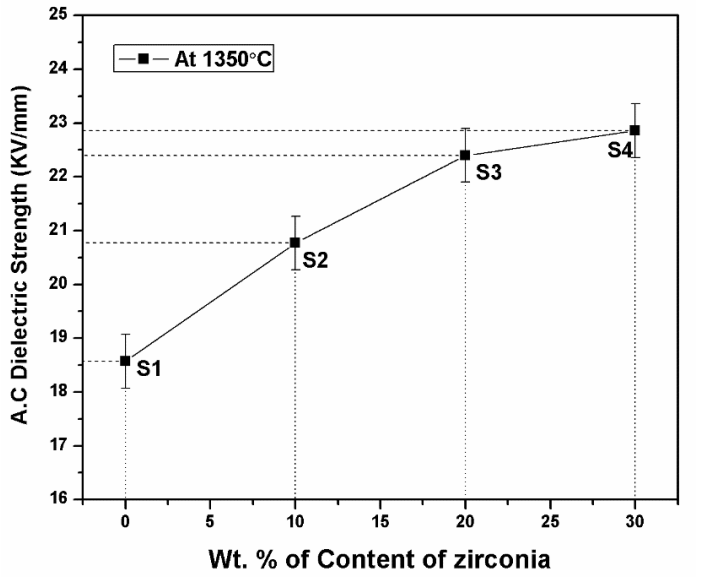

Figure 4. 16: Show the graph for dielectric strength with zirconia content.

4.4 Conclusion

In this work, an electrically and mechanically strong electrical porcelain insulator is prepared by using ZrO_2 as a substitute in low-cost clay composition by replacing alumina by weight percentage possibly for the first time. The effect of sintering temperature and ZrO_2 wt % is analyzed. XRD analysis revealed the different crystalline phase formed in sintered samples are the zircon ($ZrSiO_4$), β-cristobalite m-ZrO2, and t-ZrO2 phase. The peak intensity of β-cristobalite phase going to decreases as we increases the concentration of ZrO_2 for all the samples sintered at 1250°C and 1350°C. Samples with 20 wt. % ZrO_2 content resulted in higher bending, compressive and tensile strength, bulk density with least porosity compared to those containing 30 wt. % ZrO_2. With increasing in sintering temperature with addition of ZrO_2, the ceramic particles tends closer to each other and that influenced densification, reduction in porosity and pore size; thus vary the tensile strength of the prepared ceramic porcelain insulator. The following effects were observed when alumina was replaced with zirconia in the base electrical ceramic porcelain composition by 20 wt. % sintered at 1350°C with a soaking period of 2 hours.

- The water absorption and porosity dropped to a minimum due to the unavailability of microcracks and pores which is filled by melting glassy content of silica with zirconia-alumina composite.
- The measured value of MOR and compressive strength for PI were 138 ± 5 MPa and 221 ± 10 MPa, respectively observed.

The composition having 30 wt. % ZrO_2, dielectric constant lies in between 5.1 to 4.4 and dielectric loss 0.09 to 0.1 is measured for the frequency range of 4 to 20 GHz at room temperature for the sample sintered at 1350°C. The value of dielectric constant is observed to be increasing with the increase in ZrO_2 concentration and decreases with the

increment of the operational frequency range. As we increase the temperature, from 30° to 190°C the dielectric and loss value start increasing slowly. At 6 GHz, for all the prepared samples yield good dielectric value with minimum dielectric loss is achieved.

The maximum approximate real dielectric permittivity (ε′) value for a sintered (1350 °C) sample having ZrO_2 (30 wt. %) at 100 KHz, 1 MHz is 15, and 14.7 respectively were observed at room temperature. The value of ε′ is perceived to be increasing with ZrO_2 content and decreases with the increment of frequency (from 20 Hz to 1 MHz) range. Also, the highest observed AC dielectric strength for this composition is 22.85 ± 0.5 KV/mm, which is sintered at 1350°C.

A significant improvement in both mechanical and electrical properties makes the novel insulators useful for high voltage insulators subjected to high mechanical and electrical stress. The CPIs with zirconia content of 20 wt. % shows optimum performance considering economical aspect and improvement in electrical and mechanical properties.